Crack resistance of carbonized layer of multilayer polyurethane with nanofillers. Combination of casting, solution, carbonization by ion implantation technologies

R. I. Izyumov, A. L. Svistkov, V. S. Chudinov
Institute of Continuous Media Mechanics UB RAS, Perm 614013, Russia
izumov@icmm.ru, http://orcid.org/0000-0002-2083-039X
svistkov@icmm.ru, http://orcid.org/0000-0002-4754-5214
chudinovsl@mail.ru, http://orcid.org/0000-0003-2528-4866

I. V. Osorgina, A. G. Pelevin
Perm State University, Perm 614990, Russia
osorgina@psu.ru, pelevin@icmm.ru

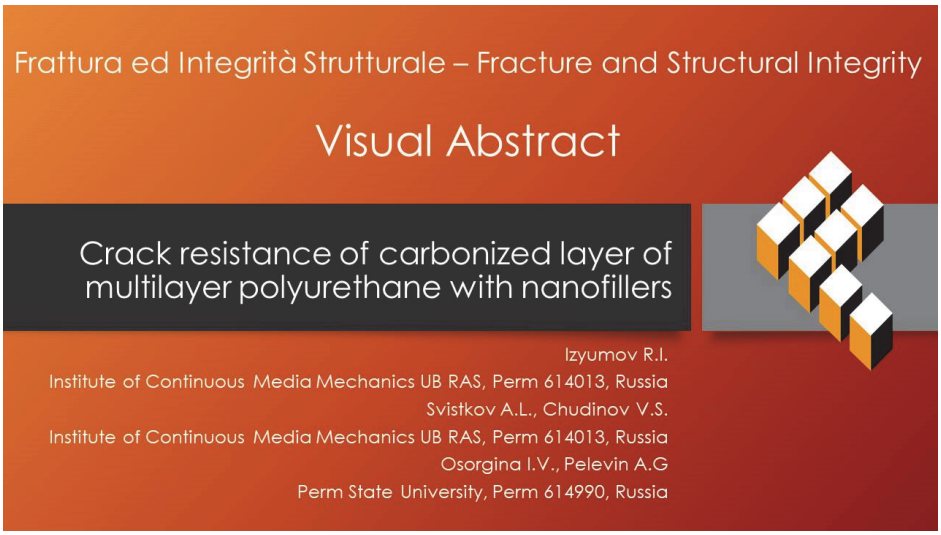

Citation: Izyumov, R.I., Svistkov, A.L., Chudinov, V.S., Osorgina, I.V., Pelevin, A.G, Crack resistance of carbonized layer of multilayer polyurethane with nanofillers. Combination of casting, solution, carbonization by ion implantation technologies, 67 (2024) 108-117.

Received: 01.08.2023
Accepted: 27.10.2023
Online first: 31.10.2023
Published: 01.01.2024

KEYWORDS. Polyurethane, Ion implantation, Carbonized layer, Cracks, Digital optical and atomic force microscopy, Nanofillers.

INTRODUCTION

In the production of medical devices made of elastic materials intended for use inside the human body there are a number of requirements aimed at reducing the probability of rejection by the organism, eliminating such negative phenomena as encapsulation, coating with excrescences and sediments. In other words, the material should be

biocompatible [1].
Polyurethane is a promising material for the manufacture of such products. Different polyurethane synthesis formulations allow obtaining a wide range of mechanical properties of this material, so polyurethanes are widely used in the manufacture of biomedical products: tubes, catheters and artificial vessels [2, 3], implants [4, 5], cellular matrices [6], interphalangeal prostheses [7], etc. The need for additional treatment is caused by the fact that polyurethane is a bioinert material, i.e., it has no toxic effect on the organism, but it is perceived as a foreign object. To ensure the conditions of compatibility with the biological tissues of the body, the possibility of modifying polyurethane, which would allow to deceive the body and hide the presence of a foreign object from it, is actively studied [8-10]. One of the stages of modification is ion treatment [11], which can be used to change the physical (surface energy [12], thermal expansion [13]), mechanical (stiffness [14], friction coefficient [15]), chemical (structural and elemental composition) and geometric (roughness and texture [14, 16]) surface characteristics. During ion implantation, the surface properties change due to ion irradiation, which results in a significant change in the near-surface layer structure [17, 18], macromolecules are destroyed, new carbon bonds are formed, and the surface layer is transformed into the so-called carbon layer [19, 20].
Such a layer contributes to the reduction of cellular infiltrates and the collagen sheath around the polymeric endoprosthesis [21], increases the sorption activity of some proteins (proteins that promote cell growth, e.g. albumin, fibronectin, which in turn provides better biocompatibility with the tissues of the organism) [22-24], decreases the activity of other proteins (fibrinogen, which accelerates thrombosis) [12, 25], improves antibacterial properties [26], allows to control blood coagulation [27], and also reduces interphase friction [28].
However, despite all the above-mentioned advantages of ion implantation treatment, the obtained carbon coatings are quite brittle [29]. Even small deformations, which should occur during the exploitation of the endoprosthesis, can cause the appearance of cracks [30]. The negative effect of cracks is that the body tissues surrounding the implant can be pinched between the edges of the crack, causing an immune reaction.
It is proposed to consider the problem not in the presence of cracks themselves, but how these cracks behave during the implant exploitation (whether there is a tendency to grow rare cracks or whether the more favorable way is to grow the number of small cracks). This approach allows those material compositions that are able to resist the formation of large, wide cracks.
In order to comply with multiple requirements to the implant, the work investigates composite materials combining different technologies of polyurethane production, as well as the use of different nanofillers and different number of layers of materials.
The work is devoted to searching for the most optimal combination of polyurethane implant production technologies.

MATERIALS AND METHODS

The polyurethane samples were produced by casting technology (designated as *C-polyurethane*). Polyurethane prepolymer EP SKU PT-74 based on simple polyester and 2,4-toluene diisocyanate (TDI) was used for polyurethane synthesis. The prepolymer was cured using a combination of curing agents including 3,3'-dichloro-4,4'-diaminodiphenylmethane (84.7% by mass), polyfuryl and Voranol RA640 (2.1% by mass).
The surface treatment of the samples was performed using nitrogen ion implantation technology. Ion treatment of the outer layer of all samples was performed at an ion energy of 20 keV with fluences of 10^{15} ions/cm^2 and 10^{16} ions/cm^2 (hereafter, symbols *a* and *b* are used for the fluence designation, respectively).
A part of the samples after ion treatment was coated with an additional thin layer of polyurethane using spin coating technology (Laurell WS 400BZ 6NPP). The material used was polyurethane produced by solution technology (designated as *S-polyurethane*) (Fig. 1). This technology was tested for its ability to meet both the requirement for mechanical properties of the implant and the requirement for resistance to crack growth.

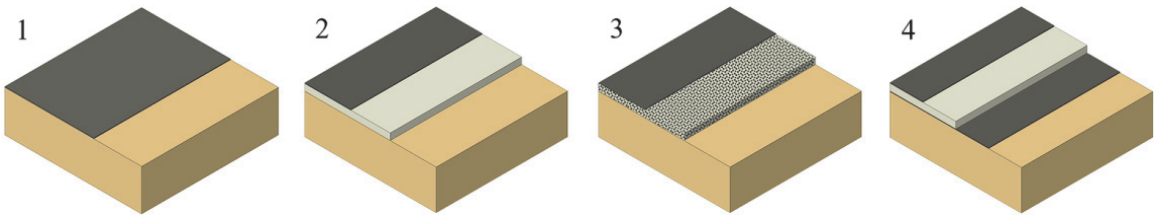

Figure 1: Types of polyurethane samples production technology.

1. C-polyurethane with a carbonized layer obtained by ion implantation treatment.
2. C-polyurethane coated with a thin (up to 10 μm) layer of S-polyurethane. S-polyurethane layer is coated with a carbonized layer.
3. It is based on the second type. Nanofiller is added to the S-polyurethane layer. The following designations are used (% denotes the mass fraction):

3-1 — 2% graphene without solvent
3-2 — 2% graphene in 50% CCl_4
3-3 — 4% graphene in 50% CCl_4
3-4 — 4% nanodiamonds in 50% CCl_4
3-5 — 2% fullerene in 50% toluene
3-6 — 3% nanotubes in 50% CCl_4

4. C-polyurethane samples with a carbonized layer coated with an S-polyurethane layer, which is also coated with a carbonized layer. The lower C-polyurethane layer is treated in two modes (10^{15} and 10^{16} ions/cm^2). The designation 4ab means that the inner (lower) layer was obtained at 10^{15} ions/cm^2 and the outer (upper) layer was obtained at 10^{16} ions/cm^2.
A special device for stretching the specimens was used to carry out the research. It allows to control the process of elongation with an accuracy of 0.1 mm. A digital optical microscope Hirox KH-7700 (HIROX, Japan) was used to obtain images of the surface at strain ε = 10, 15, 20, 30, 50, 100% and, if possible, 2.5 and 5%.
Atomic force microscopy (AFM) methods were used to study the problem of carbon layer delamination. AFM (Ntegra Prima, NT-MDT Europe BV) was used to study the relief in the area of the crack edge on the surface of the stretched sample was studied in semi-contact mode (the calibrated AFM probes were used; tip radius ~ 10 nm). It was shown that even large deformations (up to 100%) do not lead to the delamination of the carbon layer.

RESULTS

Optical microscopy

As a result of ion implantation, a wave-like relief is formed on the surface of polyurethane samples. The character of the relief is highly dependent on the manufacturing technology. Fig. 2 shows photos of the surface of all types of samples treated at a fluence of 10^{16} ions/cm^2.

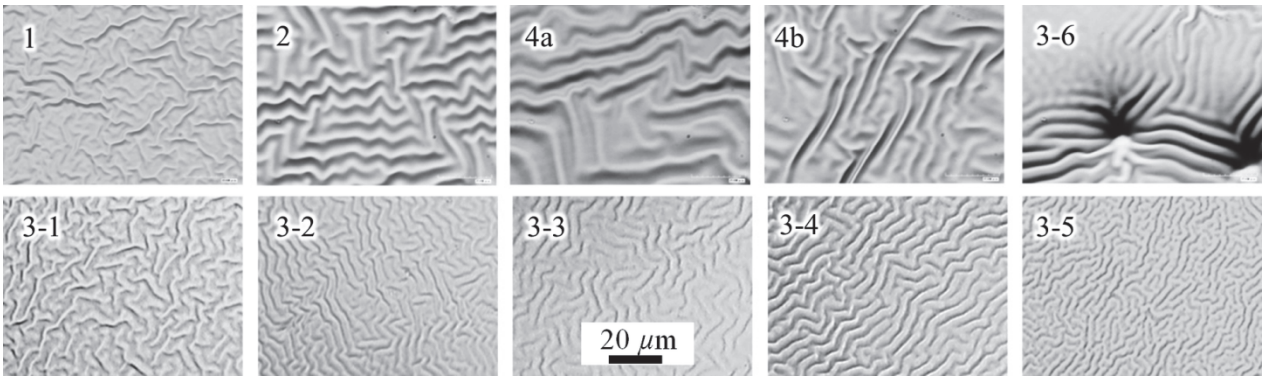

Figure 2: The surface of polyurethane samples after ion implantation at a fluence of 10^{16} ions/cm^2 and an ion energy of 20 keV.

The stretching of the samples simulates the deformations to which polyurethane should be subjected during exploitation. In the experiments, the appearance of cracks is observed, which are fixed at selected stages of stretching. Fig. 3 shows the crack growth process in the carbon layer of the samples (images have been edited).
To process optical microscope data, an algorithm is developed that includes: image preprocessing (reducing uneven brightness, blurring of image details located across cracks, selecting cracks as objects and converting the image format to binary (monochrome)). Reading the image line by line (across the cracks) allows an array of crack width values to be formed. The following parameters are proposed to evaluate the crack resistance: the modal crack width (w) and a special parameter of brittleness d (to avoid confusion, the term "crack resistance parameter" is not used because the parameter d is calculated differently: it refers to the ratio of the total crack area S_T to the area of the whole image S). The parameter d

makes it possible to distinguish between the mechanisms by which the surface is stretched (relief smoothing, crack formation).
Fig. 4 shows the crack growth as the specimen is stretched up to 100%.

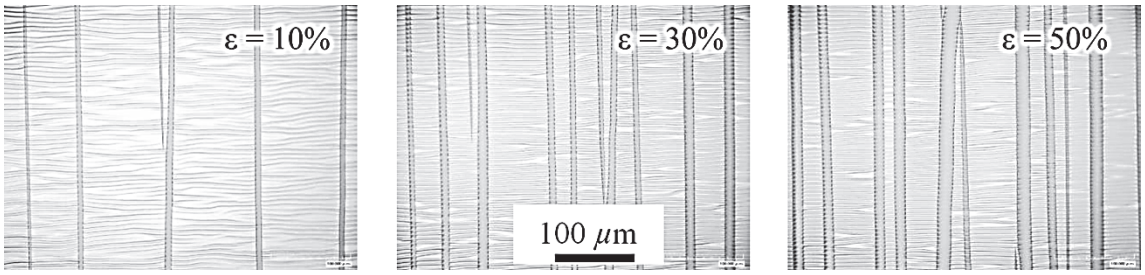

Figure 3: Surface images (the sample of type 1b) at strain ε = 10, 30, 50%. Stretching in the longitudinal direction is accompanied by compression of the specimen in the transverse direction with the formation of a wavy relief. Surface rupture is accompanied by the formation of wide crack bands in the direction transverse to the tensile direction.

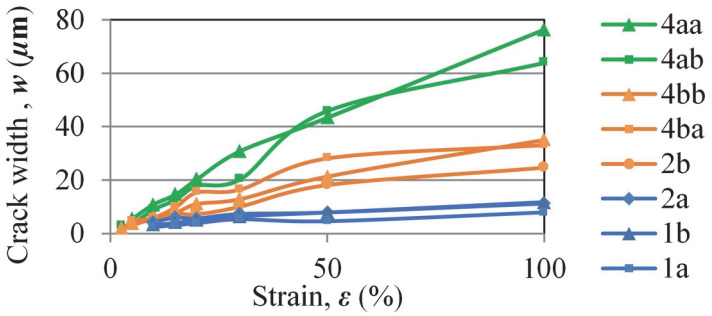

Figure 4: Dependence of crack widths on manufacturing technology at strain up to 100%.

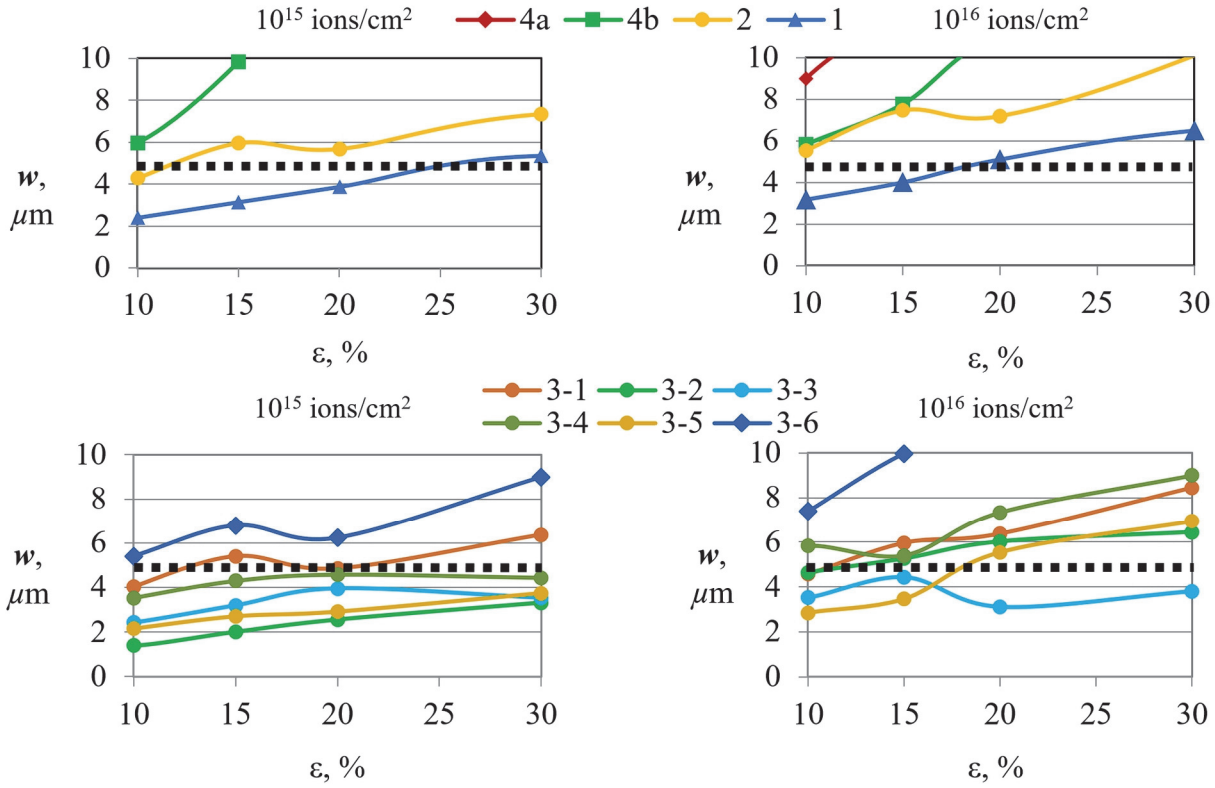

Figure 5: Dependence of crack widths on fabrication technique at strains from 10 to 30%. Left graphs: ion implantation at a fluence of 10^{15} ions/cm². Right graphs: at a fluence of 10^{16} ions/cm².

The analysis of the data obtained for the first group of samples without nanofiller revealed that the study of samples at strains more than 30% is not appropriate, because the crack width many times exceeds the established criterion (5 μm). This criterion is determined by the following reasons. It is obvious that not any cracks are dangerous for the tissues, but only those that are wider than a certain value. It is known that the cell sizes of human organ tissues vary from a size of about 5 microns (not considering cerebellar granular cells 4-4.5 microns), these are epithelial cells. Therefore, it is important to evaluate not only whether cracks exist, but how large the cracks may become when using the implant. Meanwhile, their density or the length of individual cracks do not play a significant role.

The next group of samples (with nanofiller) was studied at strains up to 30%. Fig. 5 shows graphs with the results for all the samples at the strain range from 10 to 30%.

The black dotted line indicates the criterion for the acceptable crack width - 5 μm. From the first group of samples (without filler, types 1, 2, 4) only the sample of type 1a corresponds to the chosen criterion (with a small correction). Samples with nanofillers made with solvent (3-2, 3-3, 3-4, 3-5) at a low fluence of 10^{15} ions/cm^2 fully meet the criterion (the sample 3-2 with 2% graphene has the best index). Sample 3-3 (graphene) treated with a fluence of 10^{16} ions/cm^2 is also suitable.

It was found that, in all but one case, an increase in the fluence of ion implantation treatment leads to an increase in the average crack width (Fig. 6). However, the type 4 specimen (with two carbon layers) shows the opposite tendency.

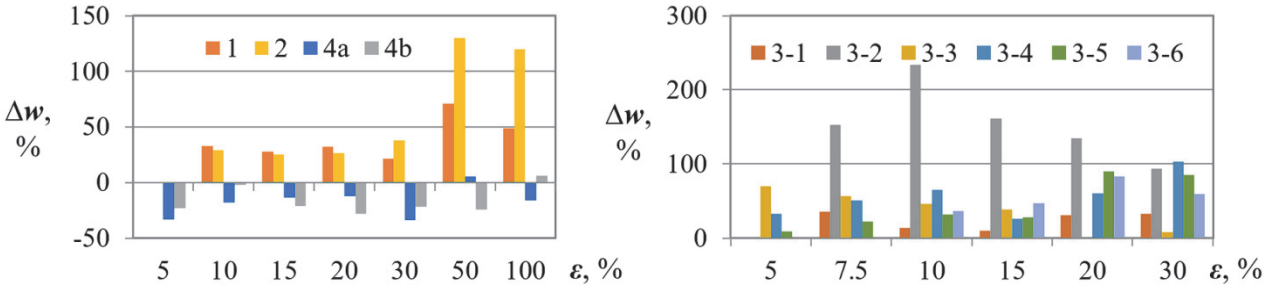

Figure 6: Relative change in the crack width as fluence is increased from 10^{15} to 10^{16} ions/cm^2.

The type 4 specimen was examined more closely. Due to the presence of the inner carbon layer, it is possible to visually distinguish the layers from each other and observe the relief of both the outer and inner layers. For this purpose, images were obtained with the focus on the lower layer and on the height *h* (Fig. 7).

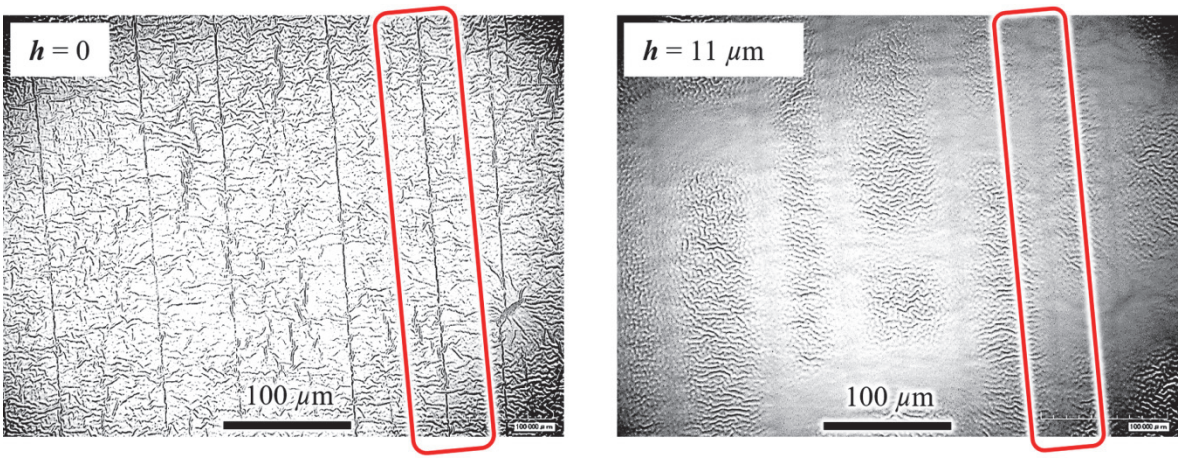

Figure 7: Photographs of the inner carbon layer (left, $h = 0$) and the outer carbon layer (right, $h = 11$ μm). The frame marks the crack on the inner layer and the concavity on the outer layer. The sample of type 4bb. Ion implantation of both layers with a fluence of 10^{16} ions/cm^2.

Cracks in the inner layer affect the formation of a large-scale relief (~100 μm wide waves) of the outer layer. This is revealed as a defocused region above the area where the crack is located (in Fig. 7, right, the wavy relief in the frame is visible blurred). It is assumed that these large waves allow the deformation of the outer surface without cracks at higher

elongation of the sample, realizing the deformation through flattening of these waves. This conclusion is confirmed by the analysis of the parameter of brittleness *d* (Fig. 8).

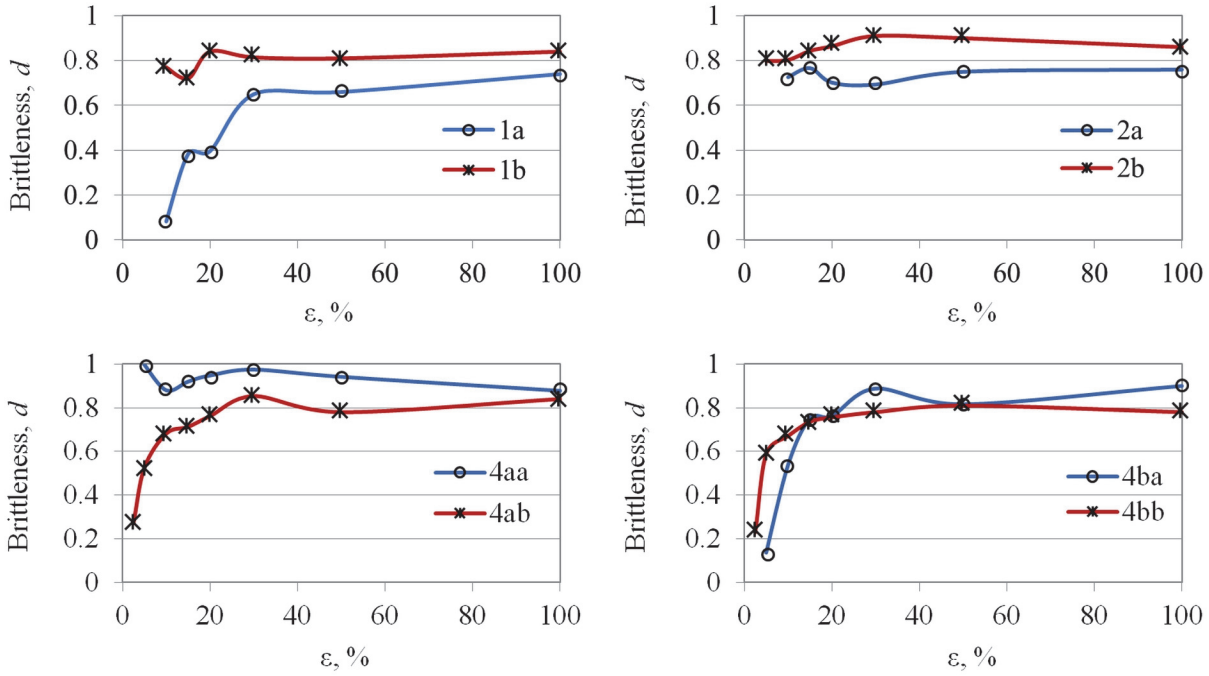

Figure 8: Samples without nanofillers. Effect of the ion fluence on the parameter of brittleness *d*. The blue line with circular markers indicates treatment with a fluence of 10^{15} ions/cm^2. Red line with crosses markers - with a fluence of 10^{16} ions/cm^2.

The parameter of brittleness *d* is close to 1 for an "absolutely" brittle layer, and close to 0 for an "absolutely" elastic surface layer. It should be noted that for type 1 and 2 samples, the treatment with increased fluence leads to material embrittlement. The parameter *d* has increased, especially in the initial stages of stretching. However, the graphs for samples of type 4 show that the layer with increased fluence becomes more elastic (4a) or maintains its elasticity at the initial stages of stretching (4b).

For the samples with nanofiller, the following conclusions were obtained: with increasing fluence a strong embrittlement of the surface layer is observed in almost all samples at small deformations. Sample 3-4 (nanodiamonds) stands out with almost complete absence of changes with increasing fluence. This sample retains the ability to realize the deformation mechanism through wave smoothing at strains up to 10%.

Calculations similar to the calculation of the parameter d are carried out in [29] on the basis of scanning electron microscopy data. However, the distance between cracks, rather than the area of cracks, is considered, which, in general, has the same essence. Analysis of the images allowed us to conclude about plastic processes in the surface layer of the material. This conclusion is reasonable if we take into account the possibility of plastic behaviour of the metallised coating and the absence of other deformation mechanisms. In general, the proposed analysis of surface images is suitable for any type of microscopy (optical, SEM, AFM).

Atomic force microscopy

An important aspect in assessing the quality of the carbon coating is its ability to resist delamination from the base substrate material during deformation. Atomic force microscopy was used to examine the relief at the crack edges on the surface of the stretched sample. Fig. 9 shows the crack relief of the sample (Type 1a) in the stretched state, ε = 30%.

All of the surface cracks in the specimens studied have a similar shape: the fracture surface first goes sharply deep into the material, and then curves smoothly to become a concave crack bottom. Usually the term "crack tip" is used in fracture theory, but in our case the tip is stretched, so it is more appropriate to use the term "bottom".

A more detailed study of the fracture surface is shown in Fig. 10.

The transformation of the structure from one type of material to another is clearly visible. This transformation area is marked with a red frame in Fig. 10. This is probably the lower boundary of the carbon layer. Thus, the thickness of the carbon layer can be determined using this technique. For this material (type 1b) and the ion implantation parameters (20

keV, 10^{16} ions/cm^2), the thickness was about 450 nm. The obtained thicknesses correlate with TRIM calculations performed by numerical simulations of the implantation of nitrogen ions into the polyurethane surface (the interaction of incoming nitrogen ions with atoms of the polymer macromolecule was described by the Wilson-Haggmark-Biersack model).

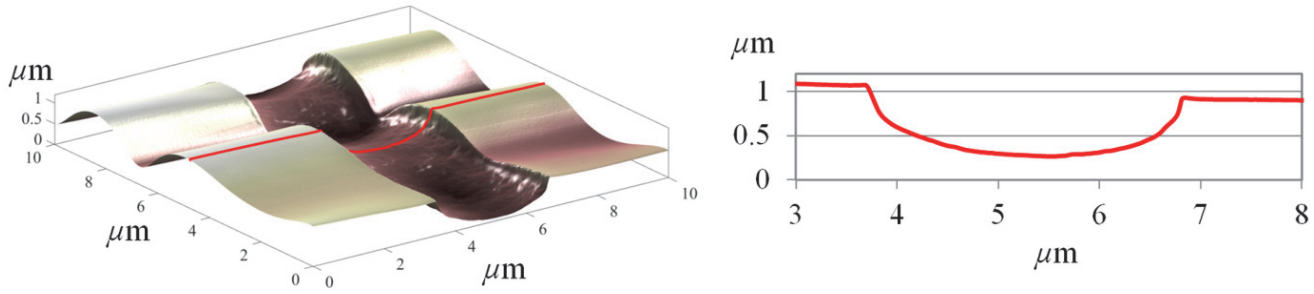

Figure 9: Crack relief of the sample (type 1a) at 30% strain. The red line indicates the surface profile shown in the right graph. Resolution of 500x500 points.

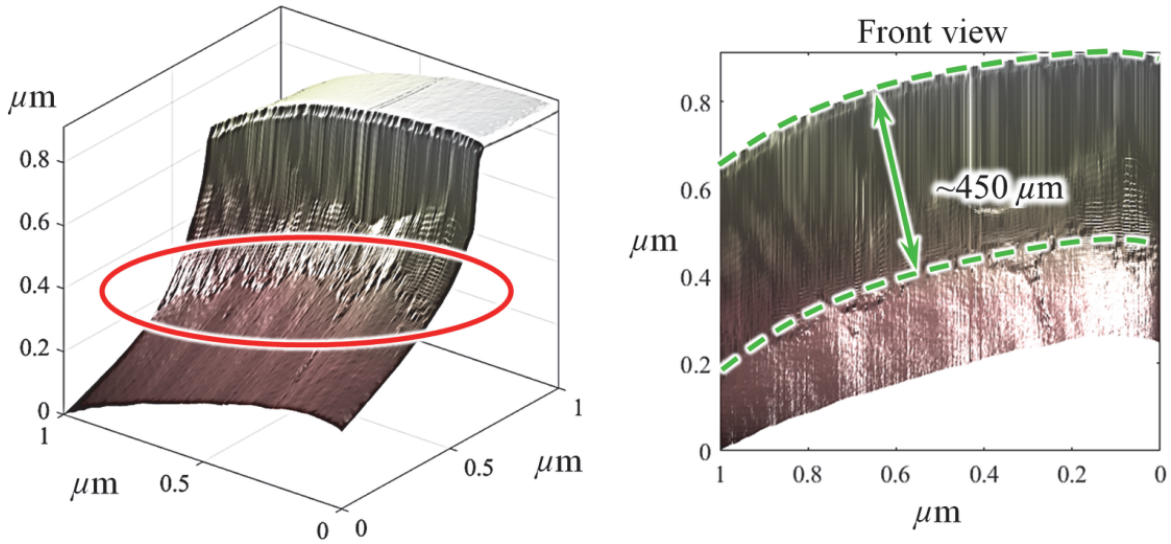

Figure 10: Fracture surface relief of the specimen (Type 1b) at 100% strain. On the left: the area where the fracture surface structure changes is marked in red. On the right: the same fracture surface, front view. The assumed boundaries (outer and inner) of the carbon layer are marked by the green dotted line. Resolution 500x500 pixels.

It is important to note the following observation (fig. 10): the transition from the carbonized layer to the polyurethane substrate is not accompanied by a sharp bending of the fracture surface, even though this region is under very high tensile loads. This suggests that there is no sharp change in mechanical properties between the two layers: they change smoothly from one material to the other. Therefore, there are no stress concentrators, which means that there are no conditions for the carbon layer to delaminate in this part of the crack either.

There is a number of works [30], in which the influence of fatigue loading on the state of carbonized polyurethane layer is investigated. The results of the substrate fracture in the area of the crack tip (bottom), the appearance of residual deformations and the evidence of stepwise ruptures of polyurethane were obtained. Presumably, this is the behavior of the material, which allows the growth of wide cracks with much larger deformations in their tips than in the variant with a large number of narrow cracks. It is important to note that the results are very sensitive to the parameters and methods of ion processing. In the given example, PIII (plasma immersion ion implantation) technology is used, and as the authors claim, the crack had a depth an order of magnitude greater than the thickness of the carbonized layer. In our case (Fig. 9, 10) the crack depth exceeds the layer thickness less than 2 times. This will also be a significant factor of crack development during implant exploitation.

DISCUSSION

The ion implantation fluence has a clear effect on almost all types of materials studied (with the exception of three-layer materials). It consists in the fact that too high a fluence (10^{16} ions/cm^2) leads to the loss of elasticity of the surface layer, which is particularly obvious for specimens produced by simple casting technology. Such a layer cannot resist deformation and it cracks.

The study of three-layer materials (type 4) has provided new data on the way to improve the quality indicators of the carbon layer. It was found that for such materials, increasing the fluence up to 10^{16} ions/cm^2 leads to an increase in the elasticity of the surface layer. This effect was shown to be associated with the appearance of large waves (~100 μm wide). Large waves allow the deformation of the outer surface without cracks at a higher degree of stretching of the sample, realizing the deformation through flattening of these waves.

The best results were obtained with material 3-2a (graphene 2%, 50% CCl_4, 10^{15} ions/cm^2). It has the narrowest cracks, which is achieved by their high density of distribution on the surface. It also has the best parameter of brittleness.

Almost all nanofillers gave a good effect at a low fluence of 10^{15} ions/cm^2. When stretching up to 30%, the crack width did not exceed the acceptable value of 5 μm. Exceptions were materials produced with solvent-free technology and with nanotubes (3-1, 3-6).

Taking into account the potential necessity of high fluence application, sample 3-3 (graphene 4%) can be considered as the most promising in this case. It has a high stability of the parameter $\boldsymbol{w}$ for any fluence and in the whole range of strain values.

Using AFM studies, it was determined that the carbon layer has good adhesion to the substrate and is not susceptible to delamination during specimen stretching. Based on the data on the relief of the crack bottom and the assumed region of the lower boundary of the carbon layer, it was found that there are no stress concentrators on them, which could contribute to further crack growth deep in the process of exploitation of the product made of such material. It follows that the crack width is also preserved, which indicates the stability of the quality of the developed material.

CONCLUSIONS

- Multilayer polyurethane samples consisting of polyurethane layers produced by casting and solution technology, carbonized polyurethane layers produced by ion implantation treatment and polyurethane layers with nanofillers were investigated. The samples were tested for resistance to crack growth on the surface of the carbon layer during their stretching.
- The proposed criterion was used to analyze the crack resistance of the samples and to determine the optimal combination of technologies for the production of polyurethane samples for medical purposes.
- Additional study on atomic force microscope showed that the obtained results will remain stable during the exploitation of the products.
- With the help of the proposed surface analysis of the samples, an explanation of the obtained results was given and the mechanism of the observed effects was described. Understanding the basic principles allows choosing the right direction for further research and technology improvement.

ACKNOWLEDGEMENTS

This work was funded by the Ministry of Science and Higher Education of the Russian Federation (theme No. AAAA-A20-120022590044-7).

REFERENCES

[1] Tsvetkova, E. A., Doroshko, E. Yu., Vinidiktova, N. S., Zotov, S. V., Shapovalov, V. M., Ukhartseva, I. Yu.,Lyzikov, A. A., Kaplan, M. L. (2022). Gelevaya kompozitsiya dlya modifitsirovaniya sinteticheskikh sosudistykh implanta-tov

[Hydrogel composition for modification of synthetic vascular implants], Polimernye materialy i tekhnologii [Polymer Materials and Technologies], 8(2), pp. 49-58. DOI:10.32864/polymmattech-2022-8-2-49-58.

[2] Kawamoto, Y., Nakao, A., Ito, Y., Wada, N., Kaibara, M. (1997). Endothelial cells on plasma-treated segmented-polyurethane: adhesion strength, antithrombogenicity and cultivation in tubes, J Mater Sci Mater Med, 8(9), pp. 551-557. DOI:10.1023/a:1018598714996

[3] Takahashi, A., Kita, R., Kaibara, M. (2002). Effects of thermal annealing of segmented-polyurethane on surface properties, structure and antithrombogenicity, J Mater Sci Mater Med, 13(3), pp. 259-264. DOI:10.1023/A:1014054716444

[4] Dulińska-Molak, I., Lekka, M., Kurzydłowski, K.J. (2013). Surface properties of polyurethane composites for biomedical applications, Appl. Surf. Sci., 270, pp. 553-560. DOI:10.1016/j.apsusc.2013.01.085

[5] Marzec, M., Kucińska-Lipka, J., Kalaszczyńska, I., Janik, H. (2017). Development of polyurethanes for bone repair, Mater Sci Eng C Mater Biol Appl., 80, pp. 736-747. DOI:10.1016/j.msec.2017.07.047

[6] Asefnejad, A., Khorasani, M. T., Behnamghader, A., Farsadzadeh, B., Bonakdar, S. (2011). Manufacturing of biodegradable polyurethane scaffolds based on polycaprolactone using a phase separation method: physical properties and in vitro assay, Int J Nanomedicine, 6, pp. 2375-2384. DOI:10.2147/IJN.S15586

[7] Beliaev, A., Svistkov, A., Iziumov, R., Osorgina, I., Kondyurin, A., Bilek, M., Mckenzie, D. (2016). Modelling of the mechanical behavior of a polyurethane finger interphalangeal joint endoprosthesis after surface modification by ion implantation, IOP Conf. Ser. Mat. Sci. And Eng., 123, 012001. DOI:10.1088/1757-899X/123/1/012001

[8] Rimpelová, S., Kasálková, N. S., Slepička, P., Lemerová, H., Švorčík, V., Ruml, T. (2013). Plasma treated polyethylene grafted with adhesive molecules for enhanced adhesion and growth of fibroblasts, Mater Sci Eng C Mater Biol Appl, 33(3) pp. 1116-1124. DOI:10.1016/j.msec.2012.12.003

[9] Popelka, A., Kronek, J., Novák, I., Kleinová, A., Mičušík, M., Špírková, M., & Omastová, M. (2014). Surface modification of low-density polyethylene with poly (2-ethyl-2-oxazoline) using a low-pressure plasma treatment, Vacuum, 100, pp. 53-56. DOI:10.1016/j.vacuum.2013.07.016

[10] Alves, P., Cardoso, R., Correia, T.R., Antunes, B.P., Correia, I.J., Ferreira, P. (2014) Surface modification of polyurethane films by plasma and ultraviolet light to improve haemocompatibility for artificial heart valves, Colloids Surf B Biointerfaces, 113, pp. 25-32. DOI:10.1016/j.colsurfb.2013.08.039.

[11] Stratanovich, V. A., Brel', D. V. (2022) Issledovanie vliyaniya obrabotki v nizkotemperaturnoy plazme tleyushchegorazryada na svoystva sopolimera metilmetakrilat-akrilonitril-butadien-stirola [Investigation of the effect of plasma-chemical treatment with low-temperature glow discharge on the properties of the methyl methacrylate-acrylonitrile-butadiene-styrene copolymer], Polimernye materialy i tekhnologii [Polymer Materials and Technologies], 8(3), pp. 74-81. DOI:10.32864/polymmattech-2022-8-3-74-81.

[12] Stueber, M., Niederberger, L., Danneil, F., Leiste, H., Ulrich, S., Welle, A., Fischer, H. (2007). Surface Topography, Surface Energy and Wettability of Magnetron-Sputtered Amorphous Carbon (a-C) Films and Their Relevance for Platelet Adhesion, Advanced Engineering Materials, 9(12), pp. 1114-1122.

[13] Jansen, F., Machonkin, M. A., Palmieri, N., Kuhman, D. (1987). Thermal expansion and elastic properties of plasma-deposited amorphous silicon and silicon oxide films, Appl. Phys. Lett., 50(16), pp. 1059-1061. DOI:10.1063/1.97969.

[14] Morozov, I. A., Mamaev, A. S., Osorgina, I. V., Beliaev, A. Y., Izumov, R. I. and Oschepkova, T. E. (2017). Soft polyurethanes treated by plasma immersion ion implantation: Structural and mechanical properties of the surface-modified layer, J. Appl. Polym. Sci., 135, 45983. DOI:10.1002/app.45983.

[15] Bismarck, A., Brostow, W., Chiu, R., Hagg Lobland, H. E. and Ho, K. K. C. (2008). Effects of surface plasma treatment on tribology of thermoplastic polymers, Polym Eng Sci, 48, pp. 1971-1976. DOI:10.1002/pen.21103.

[16] Izyumov, R. I., Chudinov, V. S., Svistkov, A. L., Osorgina, I. V., Pelevin, A. G. (2020). Influence of mechanical loads on the structure of a carbonized layer of polyurethane samples, AIP Conf. Proc., 2315(1), 050012. DOI:10.1063/5.0036781.

[17] Slepička, P., Neznalová, K., Fajstavr, D., Slepičková Kasálková, N., Švorčík, V. (2019). Honeycomb-like pattern formation on perfluoroethylenepropylene enhanced by plasma treatment, Plasma Process Polym., 16, 1900063. DOI:10.1002/ppap.201900063.

[18] Thiry, D., Vinx, N., Damman, P., Aparicio, F. J., Tessier, P. Y., Moerman, D., Leclère, P. Godfroid, T., Desprez, S., Snyders, R. (2020). The wrinkling concept applied to plasma-deposited polymer-like thin films: A promising method for the fabrication of flexible electrodes, Plasma Process Polym, 17, e2000119. DOI:10.1002/ppap.202000119.

[19] Kondyurin, A., Bilek, M. (2014). Ion Beam Treatment of Polymers, Application aspects from medicine to space. 2nd edn. Oxford, Elsevier, 268 p.

[20] Morozov, I. A., Kamenetskikh, A. S., Beliaev, A. Y., Izumov, R. I., Scherban, M. G., Kiselkov, D. M. (2022) Surface and subsurface AFM study of carbon-implanted polyurethane, Plasma Processes Polym, 19, e2100156. DOI:10.1002/ppap.202100156.

[21] Chudinov, V., Kondyurina, I., Terpugov, V., Kondyurin, A. (2019). Weakened foreign body response to medical polyureaurethane treated by plasma immersion ion implantation, Nuclear Instruments and Methods in Physics Research Section B: Beam Interactions with Materials and Atoms, 440, pp. 163-174. DOI: 10.1016/j.nimb.2018.12.026.

[22] Berlind, T., Tengvall, P., Hultman, L., Arwin, H. (2011). Protein adsorption on thin films of carbon and carbon nitride monitored with in situ ellipsometry, Acta Biomaterialia, 7(3), pp. 1369-1378. DOI:10.1016/j.actbio.2010.10.024.

[23] Kosobrodova, E. A., Kondyurin, A. V., Fisher, K., Moeller, W., McKenzie, D. R., Bilek, M. M. M. (2012). Free radical kinetics in a plasma immersion ion implanted polystyrene: Theory and experiment, Nuclear Instruments and Methods in Physics Research Section B: Beam Interactions with Materials and Atoms, 280, pp. 26-35.. DOI:10.1016/j.nimb.2012.02.028.

[24] Melnig, V., Apetroaei, N., Dumitrascu, N., Suzuki, Y., Tura, V. (2005). Improvement of polyurethane surface biocompatibility by plasma and ion beam techniques, Journal of Optoelectronics and Advanced Materials, 7(5), pp. 2521-2528.

[25] Alekhin, A. P., Boleiko, G. M., Gudkova, S. A., Markeev, A. M., Sigarev, A. A., Toknova, V. F., Kirilenko, A. G., Lapshin, R. V., Kozlov, E. N., Tetyukhin, D. V. (2010). Synthesis of biocompatible surfaces by nanotechnology methods, Nanotechnol Russia, 5, pp. 696-708. DOI:10.1134/S1995078010090144.

[26] Maas, M. (2016). Carbon Nanomaterials as Antibacterial Colloids, Materials, 9(8), 617. DOI:10.3390/ma9080617.

[27] Hauert, R. R., Thorwarth, K., Thorwarth, G. (2013). An overview on diamond-like carbon coatings in medical applications, Surface and Coatings Technology, 233, pp. 119-130. DOI:10.1016/j.surfcoat.2013.04.015.

[28] Kondyurina, I., Nechitailo, G. S., Svistkov, A. L., Kondyurin, A., Bilek, M. (2015). Urinary catheter with polyurethane coating modified by ion implantation, Nuclear Instruments and Methods in Physics Research Section B: Beam Interactions with Materials and Atoms, 342, pp. 39-46. DOI:10.1016/j.nimb.2014.09.011.

[29] Volynskii, A.L., Panchuk, D.A., Sadakbaeva, Z.K., Bol'shakova, A. V., Kechek'yan, A. S., Yarysheva, L. M., Bakeev, N. F. (2009). Formation of a regular microrelief in deformation of plasma-treated polymer films, Dokl Phys Chem, 427, pp. 133-135. DOI:10.1134/S0012501609080016.

[30] Morozov, I. A., Mamaev, A. S., Bannikov, M. V., Beliaev, A. Y., Osorgina, I. V. (2018). The Fracture of Plasma-Treated Polyurethane Surface under Fatigue Loading, Coatings, 8, 75. DOI:10.3390/coatings8020075.